# Molecular Gas in 3C 293: First Detection of CO Emission and Absorption in a Cygnus A (FR II) Type Radio Galaxy

Aaron S. Evans*, David B. Sanders† & Joseph M. Mazzarella‡

*Division of Physics, Mathematics and Astronomy, California Institute of Technology, MS 105-24, Pasadena, CA 91125, USA

†Institute for Astronomy, 2680 Woodlawn Dr., Honolulu, HI 96822, USA

‡Infrared Processing and Analysis Center, California Institute of Technology, MS 100-22, Pasadena, CA 91125, USA

**The nuclear activity in many of the most powerful radio galaxies is believed to be triggered by galaxy-galaxy mergers.[1] As the merging proceeds, molecular gas accumulates in the center of the new gravitational potential of the merging galaxies, and serves as fuel for both circumnuclear star formation and the supermassive black hole (SBH) believed to be the source powering the extended radio emission.[2,3] We report here the first detection of CO emission and absorption in a Cygnus A-type, Fanaroff-Riley[4] II radio galaxy (FR II: edge-brightened, lobe-dominated radio morphology) – the redshift 0.045 galaxy 3C 293. FR II galaxies are observed to have the highest radio luminosities of radio sources in the local universe, and comprise a large portion of the high-redshift galaxies found in radio flux-limited surveys. Thus, galaxies like 3C 293 are the low-redshift analogs of the most radio-luminous galaxies observed at cosmological distances.**

During a NRAO 12m survey of 34 nearby, far-infrared luminous radio galaxies (ASE, DBS, JMM, and J. A. Surace, manuscript in preparation), we detected CO(1→0) emission in the morphologically disturbed[1] (see also Figure 1), FR II radio galaxy 3C 293. This detection has followed many attempts by different groups[2,3,5,6,7] to detect CO emission in

this class of radio galaxy - all other CO detections to date[2,3,8,9] have been of radio compact and of lower luminosity FR I galaxies (i.e., edge-darkened radio jet morphology). The fact that FR I jets tend to be much slower ($v_{\rm jet} \lesssim v_{\rm sound}$) than FR II jets ($v_{\rm sound} < v_{\rm jet} \lesssim 0.1c$), combined with the high CO detection rate of radio compact and FR I galaxies relative to FR II galaxies suggests that the presence or absense of a dense interstellar medium may determine the speed and ultimately the morphology of the radio jet. In the context of our CO survey, two possible formation scenarios of radio galaxies are *i)* radio compact and FR I galaxies are formed by gas-rich galaxies relative to those that form FR II galaxies and *ii)* some radio compact and FR I galaxies evolve into FR II galaxies after much of the molecular gas has been consumed or cleared away. Regardless of whether one or both of these explanations are true, 3C 293, with its abundance of molecular gas and morphological irregularities, appears to bridge the gap between radio compact/FR I galaxies and FR II galaxies.

Observations of 3C 293 with the NRAO 12m telescope were made during one observing period in January 1996. The instrument setup and observing technique are identical to those described in *Evans et al.*,[6] which summarizes a CO survey of high redshift radio galaxies. The receivers were tuned to the frequency 110.35 GHz, corresponding to a redshift of 0.045[10,11] for the CO(1→0) emission line. Follow-up aperture synthesis maps of CO(1→0) and 3 mm continuum emission in 3C 293 were made with the Owens Valley Radio Observatory (OVRO) Millimeter Array in a low-resolution configuration providing a 4.0″ synthesized beam (September and October 1997), and in a high-resolution configuration providing a 2.5″ beam (November 1997).

The NRAO 12m Spectrum is shown in Figure 2. The CO emission line is moderately broad (velocity width at half the maximum intensity is $\sim$400 km s$^{-1}$; the mean value for infrared luminous galaxies[12] is $\sim$250 km s$^{-1}$) and appears to have an absorption feature at the systemic velocity. A similar H I absorption feature has been observed in 3C 293.[13]

The synthesized, continuum-subtracted CO(1→0) emission and 3 mm continuum in 3C 293 are shown in Figure 3. The CO emission appears to be distributed in an inclined, rotating disk surrounding an unresolved, embedded continuum source – presumably a black hole being fed by the accretion of molecular gas. The absorption feature seen in the 12m spectrum (Figure 2) is more apparent in the OVRO spectrum (Figure 3). The absorption is coincident with the position of the continuum source, indicating that radiation from the central engine is being absorbed by the presence of cold, molecular gas along our line of sight. Assuming that the CO covers the continuum source, the optical depth, $\tau$, of the line of sight CO can be determined by the flux density of the continuum emission, $I_{\rm cont}$, and the depth of the absorption feature, $\Delta I_{\rm abs}$, $\tau = \ln(I_{\rm cont}/(I_{\rm cont} - \Delta I_{\rm abs})) = 0.69$. This is significantly higher than the optical depth of 0.085 calculated for the H I absorption[13], but much less than the optical depth of giant molecular clouds (GMCs: $\tau > 10$), where most of the star formation in galaxies occurs.[14] Given the width of the absorption feature, $\Delta v_{\rm abs} \sim 60$ km s$^{-1}$, and assuming circular rotation, the absorption occurs in clouds at a distance of $r_{\rm cloud} = M_{\rm BH}G/\Delta v_{\rm abs}^2 \sim 120(M_{\rm BH}/10^8)$ pc from the continuum source, where $M_{\rm BH}$ is the mass of the accreting black hole and G is the gravitational constant. This is comparable to the metric size of the dust torus surrounding the nucleus of the nearby FR II radio galaxy 3C 270 (NGC 4261), detected using the Hubble Space Telescope (HST).[15] A similar dust torus ~250 pc in diameter would subtend only ~0.3″ at the distance of 3C 293, making it very difficult to resolve with current optical and near-infrared ground-based telescopes.

The CO luminosity is often expressed in units of (K km s$^{-1}$ pc$^2$) as

$$L'_{\rm CO} = 2.4 \times 10^3 \left(\frac{S_{\rm CO}\Delta v}{\rm Jy\ km\ s^{-1}}\right)\left(\frac{D_{\rm L}^2}{\rm Mpc^2}\right)(1+z)^{-1} \times [\rm K\ km\ s^{-1}\ pc^2],$$

where $S_{\rm CO}\Delta v$ is the CO flux, $D_{\rm L}$ is the luminosity distance to the galaxy, and $z$ is the redshift of the galaxy.[6] For 3C 293, $S_{\rm CO}\Delta v = 51$ Jy km s$^{-1}$ and $D_{\rm L} = 180$ Mpc, thus

$L'_{CO} = 3.8 \times 10^9$ K km s$^{-1}$ pc$^2$. To calculate the mass of molecular gas in 3C 293, we make the reasonable assumption that the CO emission is optically thick and thermalized, and that it originates in gravitationally bound molecular clouds. Thus, the ratio of the $H_2$ mass and the CO luminosity is given by, $\alpha = M(H_2)/L'_{CO} \propto \sqrt{n(H_2)}/T_b\ M_\odot$ (K km s$^{-1}$ pc$^2$)$^{-1}$, where $n(H_2)$ and $T_b$ are the density of $H_2$ and brightness temperature for the CO(1→0) transition.[14,16] We adopt a value of 4 $M_\odot$ (K km s$^{-1}$ pc$^2$)$^{-1}$ for $\alpha$, which is similar to the value determined for the bulk of the molecular gas in the disk of the Milky Way.[14] Thus, the molecular gas mass of 3C 293 is $1.5 \times 10^{10}\ M_\odot$, or $\sim$5 times the molecular gas mass of the Milky Way. Accumulation of this much gas in the central regions of the galaxy may have been caused by the collision of two gas-rich disk galaxies.

In addition to the molecular gas mass, the dynamical mass, $M_{dyn}$, of the galaxy can be calculated from the measured radius of the CO emission, $r \sim 3.5''$ (3.0 kpc), the inclination, $i \sim 60°$, and a velocity width, $\Delta v_{FWHM} \sim 400$ km s$^{-1}$:

$$M_{dyn} = \frac{r\,\Delta v^2_{FWHM}}{G \sin^2 i} = 1 \times 10^{11}\ M_\odot.$$

Thus the molecular gas mass is $\sim$10 % of the extimated dynamical mass.

The molecular disk is oriented parallel to the disk-like structure of the galaxy, but perpendicular to the large scale radio emission shown in Figure 1. Thus, the large scale structure and the CO emission are consistent with the idea that the central engine is fed by a molecular torus/accretion disk and that the radio jets escape along the axis perpendicular to the accretion disk.[17]

The structure of the inner few arcseconds of 3C 293 is more complex: Figure 1a shows a high resolution 5 GHz MERLIN map[18] superimposed on both the CO emission and an archival HST 7000Å image of the galaxy. The radio map has been placed on the CO map by assuming that the core of the 5 GHz emission is coincident with the 3 mm core. The registration of the MERLIN map with the HST 7000Å image was done by first aligning the radio knots with features observed in a recently obtained near-infrared image

of 3C 293 taken with the Near Infrared Camera and Multiobject Spectrometer (NICMOS) onboard HST (ASE *et al.*, manuscript in preparation). Such an alignment places the core of the 5 GHz emission on what appears to be the nucleus of the galaxy. Note that the general shape and orientation of the dust lanes in the 7000Å HST image is similar to that of the CO emission, and that the eastern jet appears to pass through an off-nuclear knot directly east of the dust lane. The nature of this knot will be discussed elsewhere (ASE *et al.*, manuscript in preparation).

The axis of the inner radio emission that extends 2.5″ (2.1 kpc) from the nucleus is rotated $\sim$ 30° relative to the outer 1.5 GHz radio emission, which spans 220″ (190 kpc) from the tip of the bright NW lobe to the tip of the fainter SE lobe. Indeed, the twisting of the eastern jet is apparent in the large-scale emission, which curves from the core towards the southern lobe. Such a jet morphology can be caused by either *i)* the redirection of jets from a glancing impact with a molecular cloud, or *ii)* by a second merger event or interaction, causing a warp in the galaxy, and thus shifting the radio jet axis. The first scenario is supported by the fact that the eastern jet appears to twist northward after passing the 7000Å off-nuclear knot, then southward after passing the centroid of the western CO component. At larger radii, the galactic density gradient would drive the large-scale radio emission to be perpendicular to the molecular and stellar distribution of the galaxy. However, it is difficult to reconcile this scenario with the relativistic velocity of the large-scale radio jets, as indicated by the apparent Doppler boosting (dimming) of the approaching NW (receding SE) jets (Figure 1); an impact with molecular clouds would undoubtedly cause the inner jet to lose substantial amounts of kinetic energy. The second scenario is supported by the presence of a small galaxy $\sim$ 35″ (31 kpc) southwest of 3C 293 (Figure 1) – optical images show the companion to be connected by a bridge of emission to 3C 293, as well as a tidal tail/fan that extends southwestward beyond the companion.[1] Thus, the inner radio jets may represent a more recent outburst that has collided with the

molecular disk as the jet axis rotates away from the large scale radio axis. Following *Akujor et al.*[18], if we assume a jet propagation speed of $0.1c$, the radio outburst resulting in the large scale structure occured $5 \times 10^6$ years ago, and the secondary outburst was produced only $5 \times 10^4$ years ago.

The short lifetime of the radio emission in 3C 293, combined with the short lifetime of the merger phenomenon[19] and the abundance of molecular gas in 3C 293, provide further support of the idea that the nuclear activity in radio galaxies is triggered by the merger of gas-rich galaxies.[2,3] Our observations of 3C 293 not only signify the first detection of molecular gas in an FR II radio galaxy, but also represent a detection in the only remaining major class of active galaxies (i.e., Seyfert galaxies, LINER galaxies, QSOs, quasars, compact radio galaxies, FR I radio galaxies, FR II radio galaxies) previously undetected in CO. It is believed that many of these active galaxies eventually evolve into elliptical galaxies via dynamical relaxation,[1] and that nuclear activity subsides as the interstellar gas is consumed by nuclear black holes, or turned into stars. These $10^{6-9}$ $M_\odot$ black holes, such as those found in nearby, normal elliptical galaxies and early-type spiral galaxies,[20,21] would then remain dormant until the next gas-rich interaction/merger rekindles the nonthermal activity.

1. Heckman, T. M. *et al.*, *Astrophys. J.* **311**, 526-547 (1986).

2. Mirabel, I. F., Sanders, D. B., & Kazes, *Astrophys. J.* **340**, L9-L12 (1989).

3. Mazzarella, J. M., Graham, J. R., Sanders, D. B., & Djorgovski, S., *Astrophys. J.* **409**, 170-178 (1993).

4. Fanaroff, B. L., & Riley, F. M., *Mon. Not. R. astr. Soc.* **167**, 31–35P (1974).

5. O'Dea, C. P., Baum, S. A., Maloney, P. R., Tacconi, L. J., & Sparks, W. B. *Astrophys. J.* **422**, 467-479 (1994).

6. Evans, A. S., Sanders, D. B., Mazzarella, J. M., Solomon, P. M., Downes, D., Kramer, C., & Radford, S. J. E. *Astrophys. J.* **457**, 658-670 (1996).

7. van Ojik, R. et al., *Astr. Astrophys.* **321**, 389-396 (1997).

8. Phillips, T. G. et al. *Astrophys. J.* **322**, 73-77 (1987).

9. Scoville, N. Z., Yun, M. S., Windhorst, R. A., Keel, W. C., & Armus, L. *Astrophys. J.* **485**, L21-L24 (1997).

10. Sandage, A. *Astrophys. J.* **145**, 1-5 (1966).

11. Burbidge, E. M. *Astrophys. J.* **149**, L51-L53 (1967).

12. Sanders, D. B., Scoville, N. Z., & Soifer, B. T. *Astrophys. J.* **370**, 158-171 (1991).

13. Baan, W. A. & Haschick, A. D. *Astrophys. J.* **243**, L143-L146 (1981).

14. Scoville, N. Z. & Sanders, D. B. in *Interstellar Processes* (ed. D. Hollenbach & H. Thronson) 21-48 (Reidel, Dordrecht, 1987).

15. Jaffe, W., Ford, H., Ferrarese, L., van den Bosch, F., O'Connell, R. W. *Astrophys. J.* **460**, 214-224 (1996).

16. Solomon, P. M., Downes, D., & Radford, S. J. E., *Astrophys. J.* **398**, L29-L32 (1992).

17. Blandford, R. D. in *Eleventh Texas Symposium on Relativistic Astrophysics* (ed. D. S. Evans) **422**, 303-318 (1984).

18. Akujor, C. E., Leahy, J. P, Garrington, S. T., Sanghera, H., Spencer, R. E., & Schilizzi, R. T., *Mon. Not. R. astr. Soc.* **278**, 1-5 (1996).

19. Toomre, A. in *The Evolution of Galaxies & Stellar Populations* (ed. B. M. Tinsley & R. B. Larson) 401 (Yale University Obs. 1977)

20. Kormendy, J. & Richstone, D. *Ann. Rev. Astr. Astrophys.* **33**, 581-624 (1995).

21. Kormendy, J., Bender, R., Evans, A. S., & Richstone, D. *Astr. J.* (in the press).

22. Leahy, J. P., Pooley, G. G., & Riley, J. M. *Mon. Not. R. astr. Soc.* **222**, 753-785 (1986).

**Acknowledgements.** A.S.E. thanks A. Readhead for many useful discussions and J. P. Leahy for providing the 1.5 and 5 GHz radio maps. We thank the staffs of the NRAO 12m telescope, OVRO, and the UH 2.2m telescope for their assistance. The NRAO is a facility of the National Science Foundation operated under cooperative agreement by Associated Universities, Inc. The Owens Valley Millimeter Array is supported by NSF.

Correspondence should be addressed to A.S.E. (e-mail: ase@astro.caltech.edu).

FIG. 1 Radio (1.5 GHz) image[22] of 3C 293 superimposed on the near-infrared (2.17 $\mu$m) image. The pixel scale of the near-infrared image is 0.19″/pixel. Panel a) High resolution 5 GHz MERLIN image and high-resolution CO(1→0) distribution (see Figure 3) superimposed on the 7000Å HST image. The pixel scale of the 7000Å image is 0.046″/pixel. Assuming a Hubble constant, $H_0$, of 75 km s$^{-1}$ Mpc$^{-1}$ and a deceleration parameter, $q_0$, of 0.0, 1″ corresponds to 860 parsecs for sources at a redshift of 0.045. In all images, North is up and East is to the left.

FIG. 2 NRAO 12m CO(1→0) spectrum of 3C 293. The spectrum is plotted in units of main beam brightness temperature.

FIG. 3 OVRO map of the CO(1→0) emission and 3 mm continuum emission in 3C 293. The continuum emission corresponds to a position of $13^h50^m03.24^s$ + 31°41′33.4″. The high resolution data are plotted as 60, 70, 80, 90, and 99% contours, where 60% corresponds to a 3$\sigma$ detection and 100% corresponds to a peak flux of 0.0218 Jy/beam. The low+high resolution data are plotted as 50, 60, 70, 80, 90, and 99% contours, where 50% corresponds to a 3$\sigma$ detection and 100% corresponds to a peak flux of 0.0201 Jy/beam. Spectra extracted at several positions in the CO emission show clear evidence of rotation, as well as absorption associated with the central continuum source..

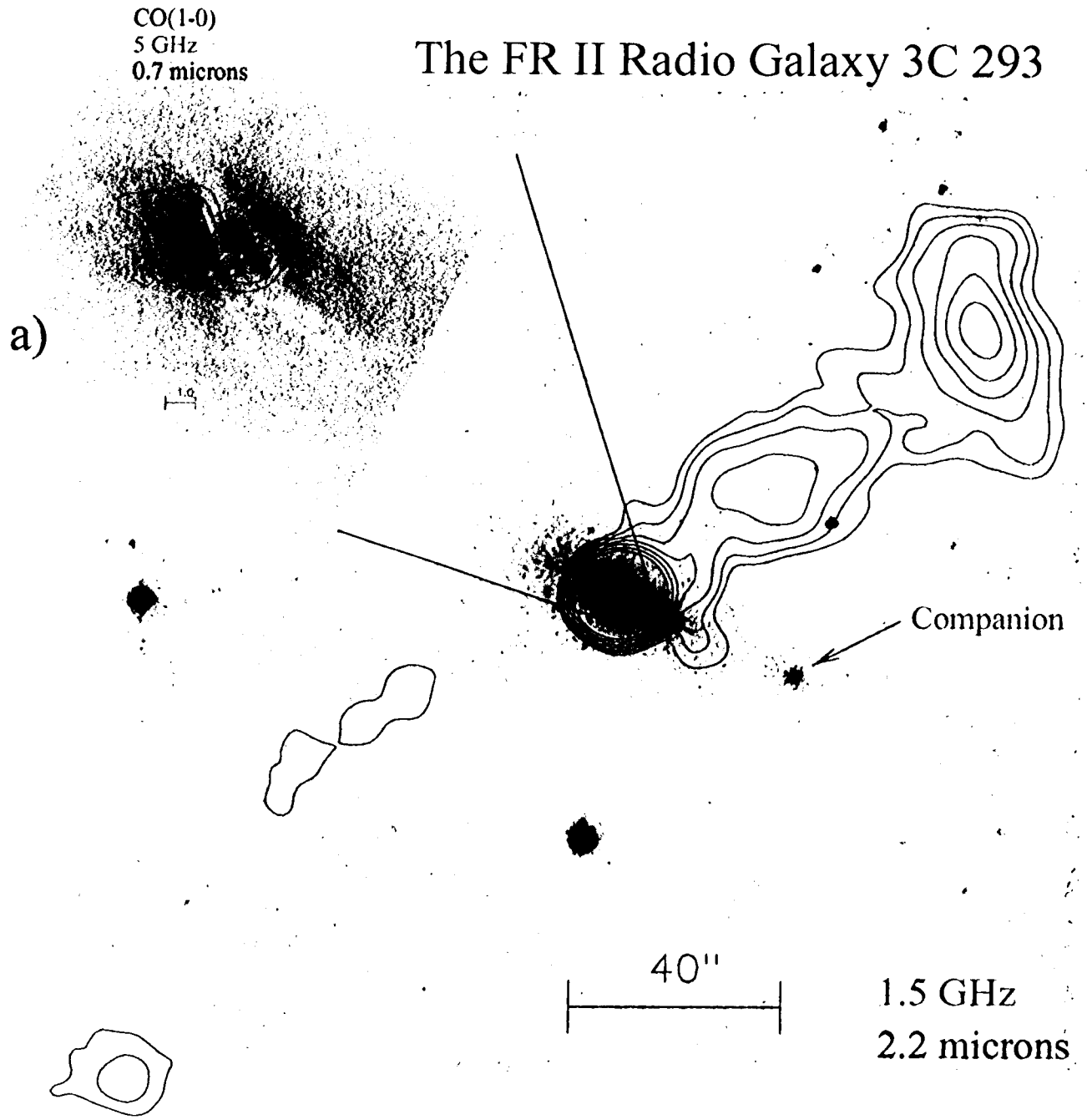


Figure 1 Evans et al

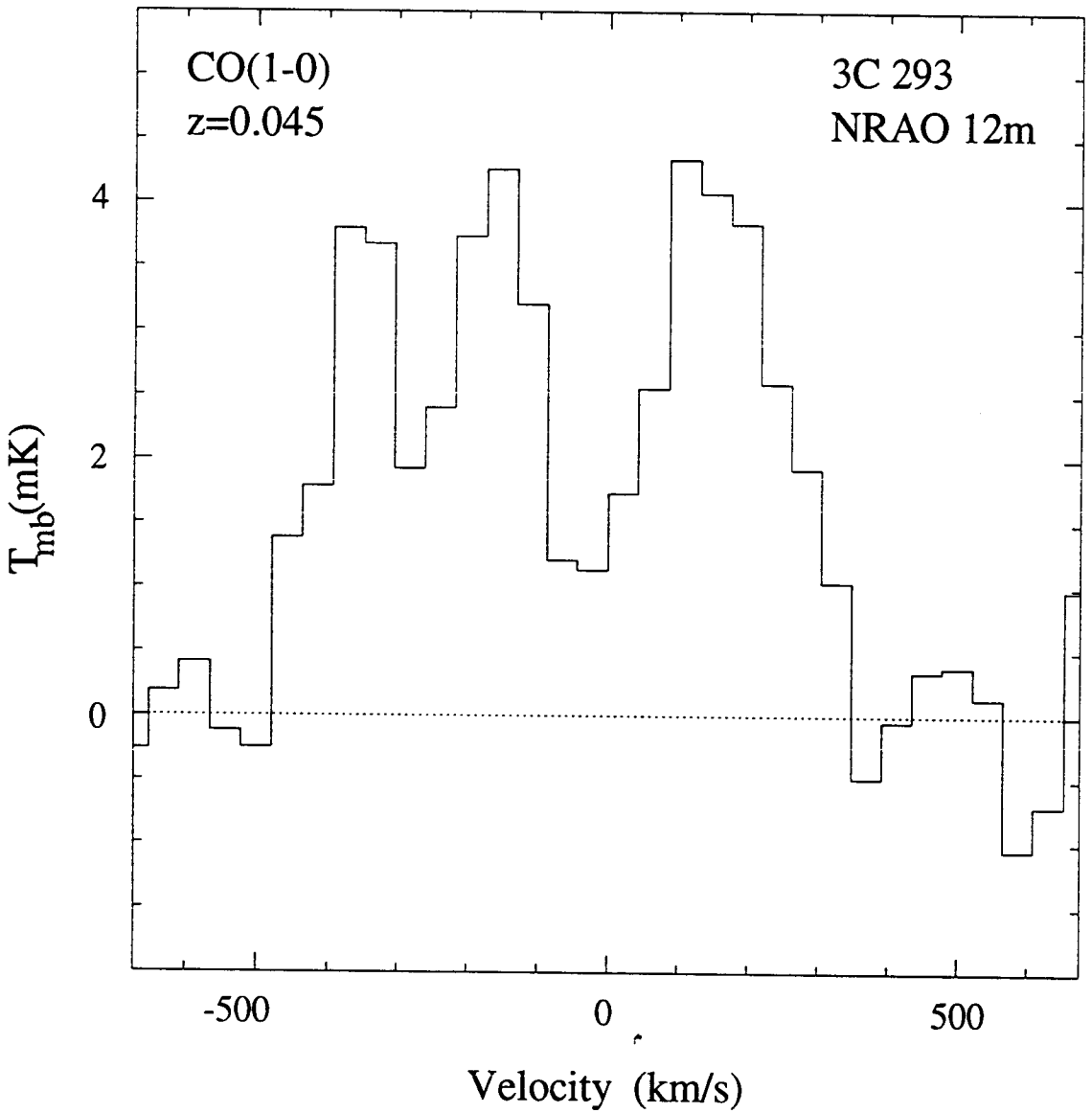


Figure 2 Evans et al.

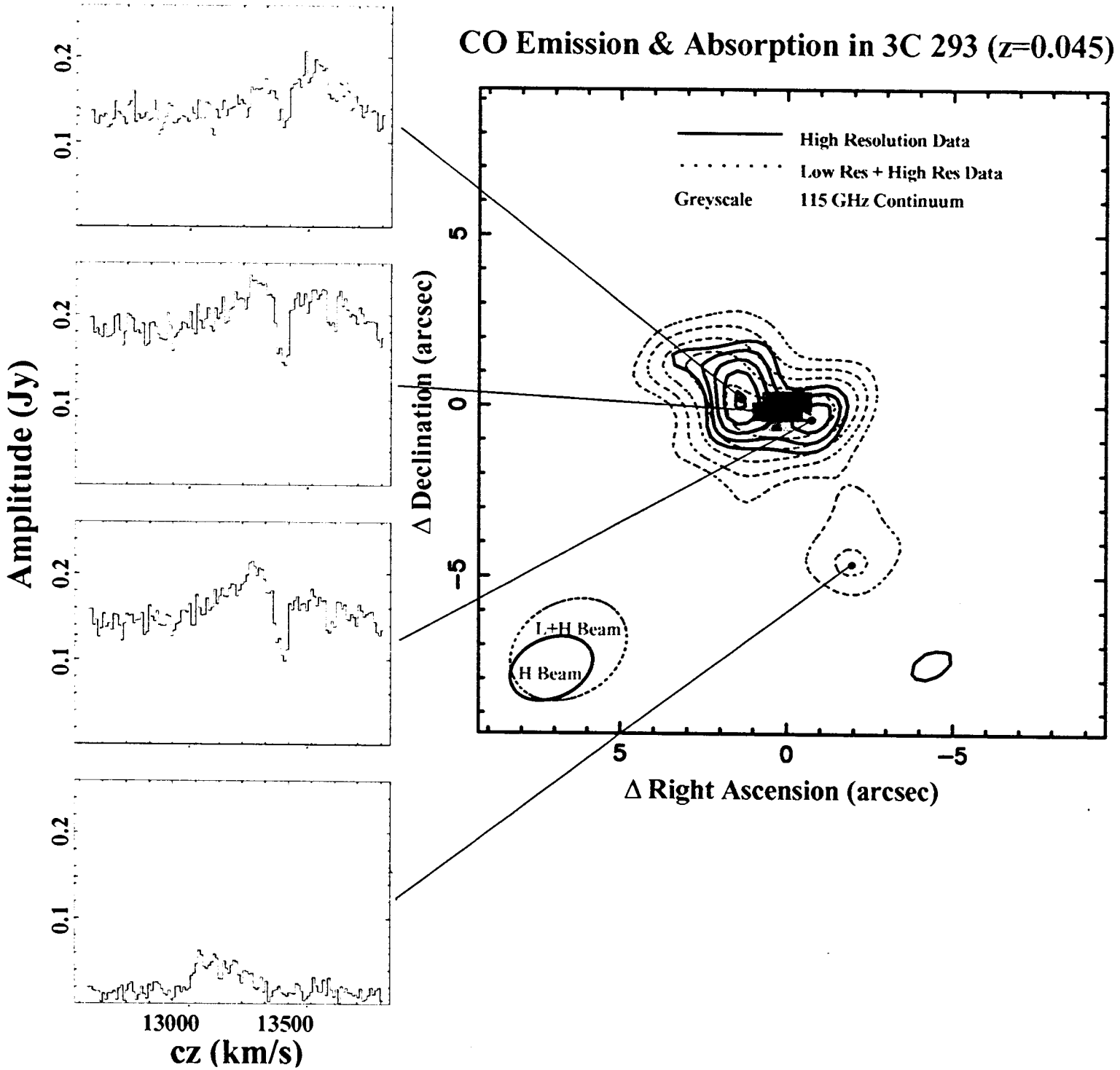


Figure 3 Evans et al.